JOURNAL OF Materials CHEMISTRY

Synthesis of novel multi-chromophoric soluble perylene derivatives and their photosensitizing properties with wide spectral response for SnO_2 nanoporous electrode

He Tian,*[a] Pei-Hua Liu,[a] Weihong Zhu,[a] Enqin Gao,[b] Da-Jun Wu[a] and Sengmin Cai[b]

[a]*Institute of Fine Chemicals, East China University of Science & Technology, Shanghai 200237, P. R. China. Fax: +86-21-64248311; E-mail: hetian@ecust.edu.cn*
[b]*College of Chemistry, Peking University, Beijing 100871, P. R. China*

Received 22nd May 2000, Accepted 4th September 2000
First published as an Advance Article on the web 26th October 2000

Two series of new multi-chromophoric perylene-3,4:9,10-tetracarboxylic dianhydride dyes for solar cell sensitizers have been synthesized. One series consists of oxadiazole or naphthaldicarboximide that are linked with perylene units as *N*,*N*′-substituted chromophores. The other series has four substituents in the bay-region of the perylene core in addition to *N*,*N*′-substituents. These novel routes to highly efficient sensitizers for Grätzel-type solar cells avoid the complication of doping. A wide spectral photoresponse (from 310 to 700 nm) was observed with maximum IPCE (incident photon-to-current efficiency) of 24%. In addition, the sensitization is dependent on the energy match of the energy bands of the semiconductor and the redox potential of the segments in such assembled dyes.

Introduction

Ruthenium(II) complexes $[Ru(L)_2(NCS)_2]$-sensitized nanocrystalline TiO_2 solar cells (Grätzel-type) with light-to-electrical power conversion efficiency as high as 10% at AM 1.5 (artificial sun light spectrum) have been reported,[1–3] in which the photoanode was prepared by sintering nanocrystalline TiO_2 on a conducting glass support. However, compared to other chromophores, the ruthenium(II) complexes have quite poor photophysics, relatively low extinction coefficients for visible light ($\sim 14000\ M^{-1}\ cm^{-1}$), and luminescence very weakly from a triplet state with a quantum yield of $\sim 0.40\%$ (125 K).[2] Furthermore, the stability of complexes such as $[Ru(L)_2(NCS)_2]$ over long-term operation in a liquid cell is unknown, which slows down the full realization of the applications of solar cells. In addition to TiO_2 used in Grätzel-type solar cells, several similar transition metal oxides (*e.g.* SnO_2)[4] with wide band gaps have also been well studied. The investigation and development of other dye-semiconductor systems are essential to furthering fundamental understanding of the electron injection processes, and exploration of specialized and long-term applications of dye-sensitized solar cell. Dyes based on perylene-3,4:9,10-tetracarboxydiimides (PTCAs) have received much attention[4] as sensitizers with their outstanding chemical, thermal and photochemical stability. Perylene derivatives are highly absorbing in the visible to NIR ($\varepsilon \sim 10^5\ M^{-1}\ cm^{-1}$) and emit fluorescence with quantum yields near unity.[5] On the other hand, perylene derivatives can also be used as near-infrared (NIR) absorbers or luminescent materials, and nowadays the highly photoluminescent and also environmentally stable NIR materials are strongly required. Beside their conventional uses, perylenes are key chromophores for high-tech applications, from electronic to biological fields, such as optical switches,[6] lasers[7] and DNA/RNA probes[8] *etc.* Many types of PTCAs have been synthesized, but the expected low solubility of these molecules is a problem for synthesis and purification. Therefore work has shifted towards more soluble perylenes.[5] The solubility of the perylene dyes may increase with attached bulky aliphatic groups like *tert*-butylaryl or long-chain secondary alkyl groups[9] (swallow-tail substituents). However, the longer alkyl and branched alkyl chain in the *N*-alkyl compounds appeared to lower the decomposition temperature. This is due to the initial decomposition of the alkyl substituent.[9b]

The bare TiO_2 or SnO_2 films are transparent and colorless, displaying the fundamental absorption in the UV region, so a solar cell with high efficiency needs efficient sensitization by a dye. The nanoporous surface of the transparent electrode is increased so that a large number of dye molecules can be adsorbed directly on the electrode surface and simultaneously be in direct contact with the redox electrolyte, which results in an efficient separation and transport of the photogenerated charge carriers. If the roughness factor of an electrode is sufficiently large, even a monolayer of dye could absorb most of the incident photons.[1] Consequently the study of a microporous electrode with a very high specific surface area and high effective sensitizers is of great interest. However, in contrast with the massive work focused on the properties of the ruthenium(II) complexes, less effort has been made so far to explore new types of organic dye sensitizers. In a new sensitizing dye–semiconductor system comprised of perylene derivatives on SnO_2, perylenes containing carboxylic acid groups adsorbed to and efficiently photosensitized colloidal SnO_2 films.[4] It is crucially important for solar cell sensitizers to control the valence band since most inorganic semiconductors such as ZnO, TiO_2 and SnO_2 exhibit n-type character.[2,4] The excited states of sensitizers must have a sufficiently long lifetime in order to undergo the photochemical reaction. The Yokoyama group found a drastic increase in the photocurrent density and the power conversion efficiency by doping H_2 due to a shift of the Fermi level.[10] A simple approach is to utilize two or more different dyes by a doping method, which shows strong absorption at a different wavelength and compensatory absorbency.[11,12] However, multilayer adsorption does not often help, as the inner layer tends to act as an insulator with respect to the outer ones.

Another possible approach is to incorporate known chromophoric units into a molecule. Such multi-chromophoric dyes should have a wide absorptive region, whose photocurrent could cover the whole visible region. The alternatives leave much scope for a chemist. In this way, it might be possible to avoid the complication of doping and to find a novel route to design appropriate solar cell sensitizers. Scandola *et al.*[13] used an appropriate antenna-sensitizer assembly to overcome

 DOI: 10.1039/b004063k

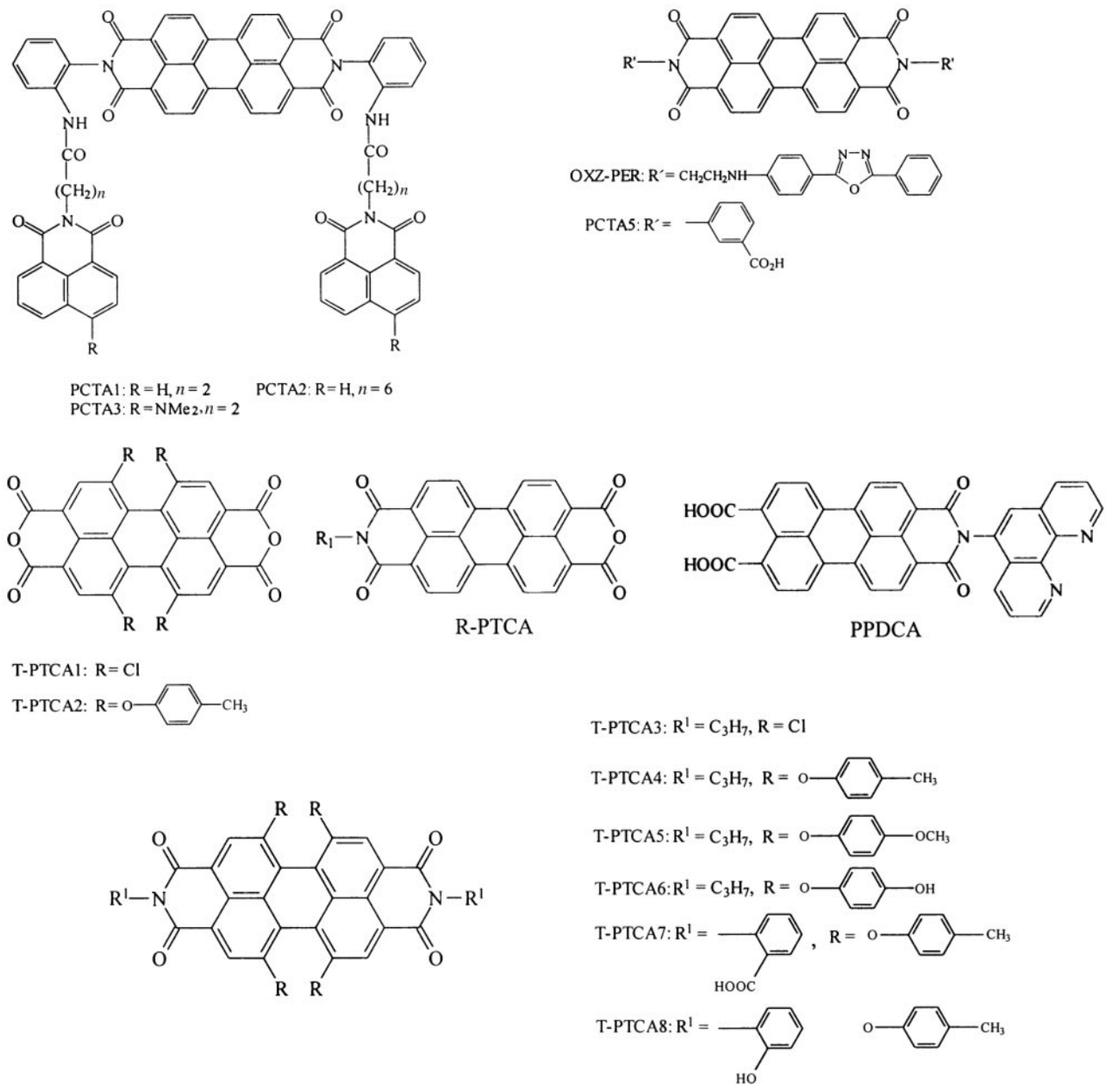

Fig. 1 The molecular structures of multi-chromophoric perylenedicarboximide derivatives.

problems of light harvesting efficiency in the spectral sensitization of wide-band gap semiconductors. As electrical and optical function rely on extended conjugated systems, two ways to enlarge the π system of perylene dyes can be envisaged:[5b] an arylimidazole introduction and substituents in the bay-region of the perylene core. The first route generally yields dyes with fairly poor solubility, and unfortunately the UV/Vis spectrum of these dyes depends weakly on the substituents.[5c] Accordingly we designed and synthesized several novel soluble multi-chromophoric dyes (perylenetetracarboxydiimide derivatives) as shown in Fig. 1. One series consists of oxadiazole or naphthaldicarboximide units that are linked with perylene units as *N*,*N*′-substituted chromophores. The other series has four substituents in the bay-region of the perylene core besides *N*,*N*′-substituents. They have long-wavelength absorption, surprisingly good solubility in organic solvents and high thermal stability. These novel routes to design highly efficient sensitizers for Grätzel-type solar cell can avoid the complication of doping. Due to the high photostability, broad visible-light absorption and high extinction coefficiency ($\varepsilon \sim 10^5\ M^{-1}\ cm^{-1}$, 450 ~ 600 nm in solution) of perylenedicarboximide derivatives, they are potentially interesting compounds for solar cells. The improved solubility of perylenedicarboximide in common organic solvents provided possible adsorption onto colloidal SnO_2 films. Naphthal-1,8-dicarboximide can absorb blue, green and yellow colors by adjusting the substituted group at its 4-position. The LUMO levels[14] of the oxadiazole unit and perylene unit are higher than that of the conduction bond (CB) of nanoporous TiO_2 or SnO_2

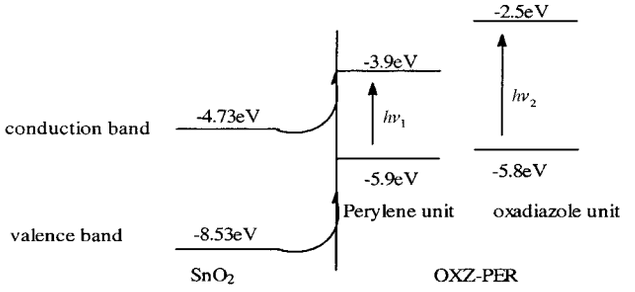

Fig. 2 Schematic representation of the band levels of SnO_2 and sensitizer OXZ-PER.

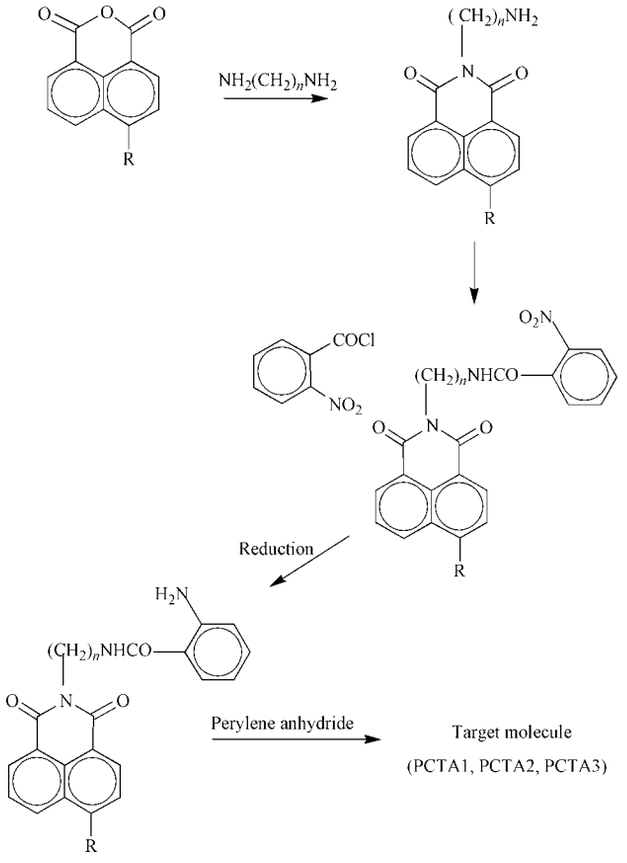

Scheme 1 Synthetic scheme of PCTA colorants.

(shown in Fig. 2). We expect that these novel multi-chromophoric sensitizers can improve the electrochemical and photostability of the Grätzel solar cells under high photocurrent density, which was the key problem limiting the practical application.

Experimental

^{1}H-NMR spectroscopy: Bruker 500 MHz (relative to TMS). Mass spectra were obtained with HP5989A, Mariner API time-of flight (TOF, TIS ion source, PE Corp.) and API2000 (TIS, PE Corp.) spectrometers. Infrared spectra were measured on a Shimidzu IR-408. UV-vis were recorded on a Shimidzu UV-260. Fluorescence spectroscopy were recorded on a HITACHI-850. Quinoline and 1-methyl-2-pyrrolidone (NMP) were distilled over calcium hydride and molecular sieves (4 Å) respectively, under reduced pressure. Methylene chloride was distilled over P_2O_5, and diphenylmethanine was used as an indicator. See Scheme 1 for representative syntheses.

Synthesis of *N*-(6-aminohexyl)naphthal-1,8-dicarboximide (I)

A mixture of naphthalic 1,8-anhydride (6.0 g, 30 mmol), hexane-1,6-diamine (69.8 g, 600 mmol) and absolute ethanol (180 ml) was stirred and heated at 80 °C, for 1.5 h, then filtered. The filtered solution was evaporated and poured into 2000 ml of water. The precipitate was filtered and dried in a vacuum to obtain 3.3 g (**I**) in 36.8% yield, mp: 78–80 °C. $C_{18}H_{20}N_2O_2$: found C 72.93, H 6.73, N 9.43; calcd C 72.97, H 6.76, N 9.46%.

Synthesis of *N*-[6-(2-nitrophenyl)carbonylaminohexyl]naphthal-1,8-dicarboximide (II)

A mixture of **I** (3.0 g, 10 mmol), 2-nitrobenzoyl chloride (2.3 g, 12 mmol), absolute THF (90 mml) and re-distilled pyridine (7 ml) was stirred at room temperature for 20 h. The end of the reaction was determined by thin layer chromatography (TLC). The reaction mixture was evaporated and poured into 300 ml of water. The resulting precipitate was filtered and crystallized from ethanol to give 2.2 g (**II**) in 67% yield, mp: 169–172 °C. MS (EI = 70 eV) *m*/*z*(%): 445(12.8) [M^+], 156(23.29). $C_{25}H_{23}N_3O_5$: found C 67.40, H 5.14, N 9.40; calcd C 67.42, H 5.17, N 9.44%.

Synthesis of *N*-[6-(2-aminophenyl)carbonylaminohexyl]naphthal-1,8-dicarboximide (III)

A mixture of **II** (1.6 g, 3.6 mmol), reduction iron powder (5.6 g, 100 mmol), absolute ethanol (150 ml) and water (60 ml) was agitated and heated to 75 °C,, then 4 ml hydrochloric acid (conc. HCl–H_2O = 1 : 3 (v/v)) was added dropwise for 2 h. TLC determined the end of the reaction . The resulting mixture was adjusted to pH = 7 by anhydrous sodium carbonate and sodium sulfide and heat filtered. The hot filtrate was cooled, filtered and dried under vacuum to obtain 1.2 g (**III**) in 80% yield, mp 167–169 °C. ^{1}H-NMR (in d_6-DMSO): δ 1.15–2.00(8H, m), 3.19(2H, t), 4.05(2H, t), 6.49(1H), 6.67(1H), 7.14(1H), 7.44(1H), 7.83(2H), 8.48(4H). MS (EI = 70 eV) *m*/*z*(%): 416(32.01) [M^+], 121(100).

Synthesis of *N*,*N*′-bis[2-[[6-(*N*′-naphthal-1,8-dicarboximidyl)hexyl]carbonylamino]phenyl]perylene-3,4:9,10-tetracarboxydiimide (PCTA2)

A mixture of *N*-[6-(2-aminophenyl)carbonylaminohexyl]-naphthal-1,8-dicarboximide (1.2 g, 2.9 mmol), perylene-3,4:9,10-tetracarboxylic dianhydride (0.3 g, 0.76 mmol), zinc acetate (0.5 g) and redistilled quinoline (25 ml) was stirred and kept at 200–215 °C, for 7 h under the protection of argon gas. Absolute ethanol (30 ml) was poured into the resulting mixture when cooled at 70 °C, and stirring was continued for 0.5 h, and then filtered to obtain a red solid. The solid was purified by refluxing with dimethylformamide and absolute ethanol, to give 0.5 g (PCTA2) in 55% yield, mp > 300 °C. IR (KBr): ψ = 3370, 3060, 2920, 2870, 1700, 1660, 1600, 1590, 1580, 1360, 1350, 810, 760, 750 cm^{-1}. ^{1}H-NMR (in CF_3CO_2D): δ 1.1–2.3(16H, m), 3.67(4H, t), 4.16(4H, t), 7.7–8.3(12H), 8.3–9.7(16H, m).

Other PCTA compounds were synthesized by a similar procedure. PCTA1: IR(KBr): ψ = 3410, 3390, 3060, 2950, 1700, 1660, 1590, 1550, 1530, 1350, 810, 780, 750 cm^{-1}. ^{1}H-NMR (in CF_3CO_2D): δ 3.9(4H, t), 4.63(4H, t), 7.51 ~ 9.15(28H, m). PCTA3: 3390, 3070, 2950, 1700, 1660, 1590, 1570, 1550, 1350, 810, 780, 760, 750 cm^{-1}. ^{1}H-NMR (in CF_3CO_2D): δ 3.9(12H, s), 4.08(4H, t), 4.78(4H, t), 7.71(2H, d), 7.91(2H, d), 8.20(4H, m), 8.32(2H, d), 8.43(2H, m), 8.85 ~ 9.08(14H, m). OXZ-PER: IR(KBr): ψ = 3380, 3040, 2920, 1690, 1660, 1610, 1590, 1500, 1340, 805, 780, 750 cm^{-1}.

The synthesis of the T-PTCA series starts with tetrachloroperylene tetracarboxylic dianhydride T-PTCA1. Compounds T-PTCA2 and T-PTCA4 were easily obtained according to the literature procedure.[15] Condensation of T-PTCA2 with the dyes T-PTCA7, T-PTCA8 occurs cleanly in hot quinoline with zinc acetate as a catalyst, and both the C-shaped isomers and S-shaped isomers were obtained as deep red compounds. The clefts were already highly preorganized, not only by restricted rotation about the C(aryl)–N(imide) bond but also by fixing of the C(acid) or O(-OH)–C(aryl) bond by an internal hydrogen bond, and they could be identified by the higher polarity of the C-isomers as evidenced by a lower R_f on silica gel.[16] We have synthesized the compound $R^1 = CH_2CH_2OH$, but its solubility was not satisfactory, and when $R^1 = H$, the solubility was even worse. Demethylation of T-PTCA5 was achieved in dry methylene chloride in the presence of BBr_3. The best reaction occurred at room temperature for 12 hours and then reflux for a further 2 h. 1,6,7,12-Tetrakis(4-methylphenoxy)perylene-3,4:9,10-tetracarboxylic dianhydride (T-PTCA2): ^{1}H-NMR ($CDCl_3$):

δ 8.12(s, 4H, per), 7.11(d, 8H, $J=8.23$ Hz, Ph), 6.85(d, 8H, $J=8.39$ Hz, Ph), 2.35(s, 12H, -CH_3). *N,N′*-Dipropyl-1,6,7,12-tetrakis(4-methylphenoxy)perylene-3,4:9, 10-tetracarboxydiimide (T-PTCA4): ^{1}H-NMR($CDCl_3$): δ 8.13(s, 4H, per), 7.08(d, 8H, $J=8.19$ Hz, Ph), 6.84(d, 8H, $J=8.43$ Hz, Ph), 4.07(t, 4H, –CH_2N<), 2.33(s, 12H, –CH_3), 1.75(m, 4H, –CH_2–), 0.98(t, 6H, –CH_3).

Synthesis of *N,N′*-bis(2-carboxyphenyl)-1,6,7,12-tetrakis-(4-methylphenoxy)perylene-3,4:9,10-tetracarboxydiimide (T-PTCA7)

T-PTCA2 (0.3 g, 0.37 mmol), *o*-aminobenzoic acid (0.5 g, 3.7 mmol) and zinc acetate hydrate (0.02 g, 0.2 mmol) were added to 10 ml of dry quinoline. The reaction mixture was stirred at 190 °C, over 8 h in an argon atmosphere. After cooling to room temperature, the reaction mixture was poured in 80 mL of a 10% HCl solution in water. A precipitate appeared, which was washed with water and dried under vacuum (P_2O_5). Column chromatography (silica gel, first methylene chloride : acetone = 3 : 1, then methylene: ethanol = 6 : 1) yielded two isomers, S (higher R_f, 117 mg, 30%) and C (lower R_f, 113 mg, 29%), as deep red solids. C-isomer: mp > 300 °C; IR(KBr): $\psi=3447$, 2921, 1706, 1671, 1590, 1502, 1412, 1342, 1320, 1285, 1201 cm^{-1}; ^{1}H-NMR (500 MHz, acetone-d_6): δ 8.08(dd, 2H, $J=8.03$, 1.47 Hz, Ph), 7.88 (s, 4H, per), 7.74(m, 2H, Ph), 7.59(m, 2H, Ph), 7.45(d, 2H, $J=7.86$ Hz, Ph), 7.20 (d, 8H, $J=8.05$ Hz, Ph), 6.96(d, 8H, $J=8.14$ Hz, Ph), 2.09(s, 12H, –CH_3); $C_{66}H_{42}N_2O_{12}$ (1054.7): found C 74.99, H 3.64, N 3.21; calcd C 75.16, H 3.98, N 2.66%; Absorption peaks (in acetone) λ^{Ab}_{max}/nm(log ε): 569.8(4.61), 531.6(4.40), 438.0(4.13); Fluorescence peaks λ^{max}_{em}(in acetone, excited at 569.8 nm) = 603.4 nm; S-isomer: mp > 300 °C,; IR(KBr): $\psi=3431$, 2920, 1705, 1671, 1591, 1500, 1412, 1342, 1320, 1285, 1201 cm^{-1}; ^{1}H-NMR(500 MHz, acetone-d_6): δ 8.08(dd, 2H, $J=7.91$, 1.35 Hz, Ph), 7.85(s, 4H, per), 7.74(m, 2H, Ph), 7.59(m, 2H, Ph), 7.44(d, 2H, $J=7.83$ Hz, Ph), 7.20(d, 8H, $J=8.46$ Hz, Ph), 6.96(d, 8H, $J=8.39$ Hz, Ph), 2.09(s, 12H, –CH_3); $C_{66}H_{42}N_2O_{12}$ (1054.7): found C 75.10, H 3.63, N 3.19; calcd C 75.16, H 3.98, N 2.66%; Absorption peaks (in acetone) λ^{Ab}_{max}/nm(log ε): 569.8(4.61), 531.6(4.40), 438.0(4.13); Fluorescence peaks λ^{max}_{em}(in acetone, excited at 569.8 nm) = 603.4 nm.

Synthesis of *N,N′*-bis(2-hydroxyphenyl)-1,6,7,12-tetrakis(4-methylphenoxy)perylene-3,4:9,10-tetracarboxydiimide (T-PTCA8)

Reaction conditions and workup were similar to those for T-PTCA7, but *o*-aminophenol was used instead of *o*-aminobenzoic acid, and the reaction temperature was lowered to 180 °C. Purification was carried out by chromatography (silica gel, first methylene chloride : acetone = 25 : 1, then methylene chloride : acetone = 15 : 1). Two isomers were yielded, S (higher R_f, 103 mg, 28%) and C (lower R_f, 92 mg, 25%), as deep red solids. C-isomer: mp > 300 °C; IR(KBr): $\psi=3380$, 2920, 1705, 1668, 1585, 1460, 1410, 1342, 1286, 1200 cm^{-1}; ^{1}H-NMR(500 MHz, acetone-d_6): δ 8.05(s, 4H, per), 7.36(s, 2H, Ph), 7.27(m, 2H, Ph), 7.19(d, 8H, $J=7.81$ Hz, Ph), 7.02(d, 2H, $J=9.83$ Hz, Ph), 6.97(d, 8H, $J=8.33$ Hz, Ph), 6.91(m, 2H, Ph), 5.64(s, 2H, –OH), 2.31(s, 12H, –CH_3); $C_{64}H_{42}N_2O_{10}$ (998.6): found C 76.19, H 4.03, N 2.60; calcd C 76.97, H 4.21, N 2.81%; Absorption peaks (in acetone) λ^{Ab}_{max}/nm(log ε): 568.6(4.61), 529.6(4.40), 436.60(4.15); Fluorescence peaks λ^{max}_{em}(in acetone, excited at 568.6 nm) = 601.4 nm; S-isomer: mp > 300 °C; IR(KBr): $\psi=3378$, 2920, 1705, 1668, 1585, 1460, 1410, 1342, 1286, 1200 cm^{-1}; ^{1}H-NMR (500 MHz, acetone-d_6): δ 8.04(s, 4H, per), 7.36(s, 2H, Ph), 7.27(m, 2H, Ph), 7.17(d, 8H, $J=7.81$ Hz, Ph), 7.02(d, 2H, $J=9.83$ Hz, Ph), 6.96(d, 8H, $J=8.33$ Hz, Ph), 6.91(m, 2H, Ph), 5.64(s, 2H, –OH), 2.31(s, 12H, –CH_3); $C_{64}H_{42}N_2O_{10}$ (998.6): found C 76.28, H 4.11, N 2.60; calcd C 76.97, H 4.21, N 2.81%; Absorption peaks(in acetone) λ^{Ab}_{max}/nm(log ε): 568.6(4.61), 529.6(4.40), 436.6(4.15); Fluorescence peaks λ^{max}_{em}(in acetone, excited at 568.6 nm) = 601.4 nm.

Synthesis of *N,N′*-dipropyl-1,6,7,12-tetrakis-(4-methyloxyphenoxy)perylene-3,4:9,10-tetracarboxydiimide (T-PTCA5)

Diimide T-PTCA3 (0.5 g, 0.82 mmol), *p*-hydroxyanisole (1.01 g, 8.2 mmol) and K_2CO_3 (1.13 g, 8.2 mmol) were added to 12 ml NMP. The mixture was stirred under argon at 130 °C, for 8 h. After cooling to room temperature, the reaction mixture was poured under stirring into 100 mL of a 10% (vol) HCl solution in water. A precipitate appeared, which was washed with water and dried under vacuum (P_2O_5). Purification by chromatography (SiO_2, methylene chloride : acetone = 30 : 1) and recrystallization from $CHCl_3$–MeOH afforded 0.56 g of the title compound as a purple red powder with a yield of 71%. mp > 300 °C; IR(KBr): $\psi=3435$, 2960, 1696, 1657, 1588, 1502, 1439, 1353, 1290, 1252, 1204, 1036 cm^{-1}; ^{1}H-NMR($CDCl_3$): δ 8.10(s, 4H, per), 6.92(d, 8H, $J=9.04$ Hz, Ph), 6.83(d, 8H, $J=9.06$ Hz, Ph), 4.07(t, 4H, –CH_2N<), 1.69(m, 4H, –CH_2–), 0.95(t, 6H, –CH_3); $C_{58}H_{46}N_2O_{12}$ (962.2): found C 71.08, H 4.87, N 2.88; calcd C 72.36, H 4.78, N 2.91%; Absorption peaks(in acetone) λ^{Ab}_{max}/nm(log ε): 575.6(4.40), 535.6(4.17), 447.4 (3.90); Fluorescence peaks λ^{max}_{em}(in acetone, excited: 575.6 nm) = 607.4 nm.

Synthesis of *N,N′*-dipropyl-1,6,7,12-tetrakis-(4-hydroxyphenoxy)perylene-3,4:9,10-tetracarboxydiimide (T-PTCA6)

T-PTCA5 (0.2 g, 0.21 mmol) was dissolved in 15 ml dry methylene chloride and cooled in an acetone–dry ice bath at −80 °C. Boron tribromide (0.08 mL) was added carefully to the stirred solution. When the addition was complete, a calcium chloride tube was fitted to the top of the air condenser. The reaction mixture was allowed to attain room temperature overnight with stirring and then refluxed for a further 2 h. After cooling to room temperature, the reaction mixture was hydrolyzed by careful shaking with 10 ml of water, and then extracted with ether. The organic phase was dried over anhydrous magnesium sulfate. Purification by chromatography (SiO_2, methylene chloride : acetone = 2.5 : 1) afforded 56.2 mg of the title compound as a purple red powder with a yield of 62%. Mp > 300 °C; IR(KBr): $\psi=3380$, 2922, 1691, 1653, 1585, 1502, 1438, 1365, 1298, 1263, 1200, 1095, 1038 cm^{-1}; ^{1}H-NMR(acetone-d_6): δ 8.00(s, 4H, per), 6.95 (d, 8H, $J=8.62$ Hz, Ph), 6.86 (d, 8H, $J=8.63$ Hz, Ph), 5.64(s, 4H, –OH), 4.0(t, 4H, –CH_2N<), 1.66(m, 4H, –CH_2–), 0.92 (t, 6H, –CH_3); $C_{54}H_{38}N_2O_{12}$(906.5): found C 70.93, H 4.01, N 5.43; calcd C 71.54, H 4.19, N 5.60%; Absorption peaks (in acetone) λ^{Ab}_{max}/nm(log ε): 579.6(4.55), 537.6(4.48), 448.8(4.32); Fluorescence peaks λ^{max}_{em}(in acetone, excited: 579.6 nm) = 613.9 nm. Compounds R-PTCA[17] and PPDCA[4] shown in Fig. 1 were used as comparisons in this study.

Photoelectrochemical experiments

As shown in Fig. 3, the liquid junction solar cell for measuring the photocurrent is composed of the sensitized nanoporous SnO_2 electrode and a counter electrode with a electrolyte solution containing 0.3 mol l^{-1} LiI and 0.03 mol l^{-1} I_2 dissolved in 1,2-propylene carbonate solution. The counter electrode is saturated calomel electrode (SCE). All the potentials measured in this article are relative to SCE unless otherwise stated. SnO_2 colloids were prepared according to the method described previously.[18] Colloidal SnO_2 solution (*ca.*

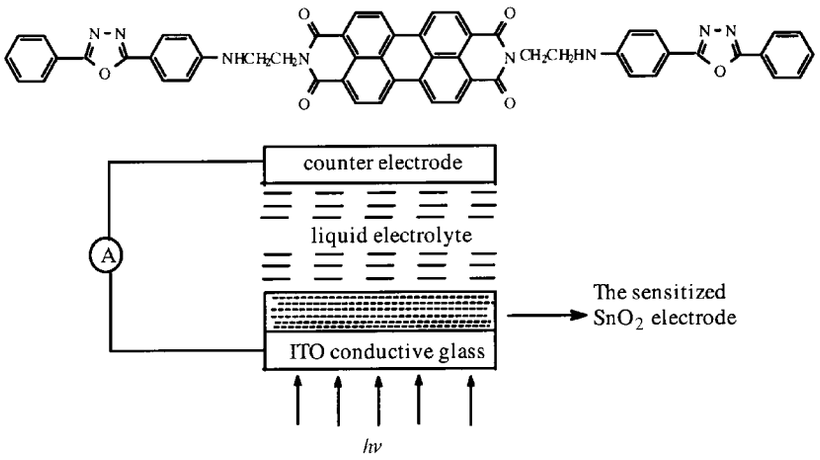

Fig. 3 Scheme of liquid junction cell based on the SnO_2 electrode sensitized by OXZ-PER.

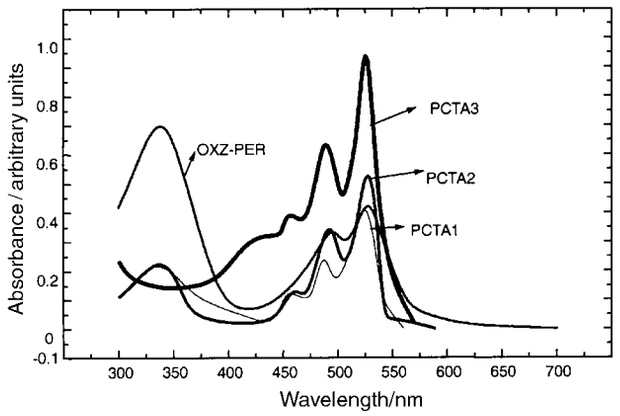

Fig. 4 Absorption spectra of PCTA1, PCTA2, PCTA3 and OXZ-PER in DMF (10^{-5} mol l^{-1}).

13%) was spread on the OTE (sheet resistance $\sim 8\ \Omega\ cm^{-2}$). After it was sintered at 250 °C for 30 minutes and the temperature dropped to about 100 °C, it was quickly immersed into saturated dye solution in DMF, kept for 24 h and then dried in air. The two-electrode sandwich cells were prepared by placing the counter electrode, a Pt plate, on top of OTE–SnO_2 or OTE–SnO_2–Dye with a thin strip of PTFE as spacer and were used to measure IPCE (Incident photon-to-current conversion efficiency).[2] The illuminated area of working electrode was 0.2 cm^2. A high-pass filter (>350 nm) was used to remove ultraviolet radiation. A potentiostat (Model 173 EG&G PARC) served to control potential. The intensities of monochromatic light were measured with a calibrated radiometer/photometer (Model 550-1, EG&G PARC). The photocurrent spectra were normalized after subtracting the transmittance of the OTE. With our preparation and measurement system, the IPCE value for *cis*-$(SCN)_2$ bis(2,2′-bipyridyl-4,4′-dicarboxylate) ruthenium(II) alone (TiO_2 electrode) was 80% in the wavelength range between 510 and 570 nm. The atomic force microscopy (AFM, DI Nanoscope III A) image indicated the morphology of the SnO_2 film deposited on a conducting glass support. It can be estimated that the SnO_2 particles in the film are spherical with the diameter of about 5 nm, so the characteristics of the SnO_2 film are nanocrystalline, and is composed of interconnected particles and pores.

Results and discussion

Absorption and fluorescence spectra

The absorption spectra of these multi-chromophoric compounds (PCTA series and OXZ-PER) in DMF are shown in Fig. 4. Comparison with the absorption of 1,3,4-oxadiazole and perylenetetracarboxydiimide, the high absorption coefficient at the wavelength of ultraviolet region (340 nm) corresponds to the absorption of the oxadiazole unit, and the peaks of 439, 529 nm correspond to the absorption of the perylene unit. That is to say the absorbency of multi-chromophoric dye OXZ-PER is the exact sum of the constituent chromophores. This means that there is little or no interaction between the chromophores connected by saturated covalent bonds in their ground state, so that their individual absorption characteristics should be maintained for OXZ-PER. For the PCTA series, the characteristic absorption of the perylene unit and naphthal-1,8-dicarboximide units were also observed. Naphthal-1,8-dicarboximide can absorb blue, green and yellow colors by adjusting the substituted group at its 4-position.[19,20] When its 4-position substituent was a dimethylamino group, *i.e.* PCTA3, the maximum absorption of the naphthal-1,8-dicarboximide was at around 430 nm, which overlaps with some of the absorption of perylene. From this standpoint, it can be shown that multi-chromophoric dyes, in which the chromophoric units are connected by saturated bonds, provide an appropriate route to effective sensitizers for solar cells with a wide spectrum range of absorption.

Absorption spectra of the perylene derivatives of the T-PTCA series are reported in Table 1. The absorption spectral data of the two isomers each of T-PTCA7 and of T-PTCA8 are

Table 1 Absorption data for the T-PTCA series in acetone (10^{-5} mol l^{-1}) and on solid film

Compounds	Absorption peaks/nm (logε)			Absorption /nm (solid film)
T-PTCA4	569.8 (3.93)	530.0 (3.72)	441.0 (3.49)	579.0
T-PTCA3	565.2 (4.03)	535.4 (3.79)	434.6 (3.64)	580.6
T-PTCA7	569.8 (4.61)	531.6 (4.40)	438.0 (4.13)	630.4
T-PTCA8	568.6 (4.61)	529.6 (4.40)	436.6 (4.15)	619.8
T-PTCA5	575.6 (4.40)	535.6 (4.17)	447.4 (3.90)	580.0
T-PTCA6	579.6 (4.55)	537.6 (4.48)	448.8 (4.32)	620.4
R-PTCA[9b]			485	
PPDCA (NMP)[4b]		514		

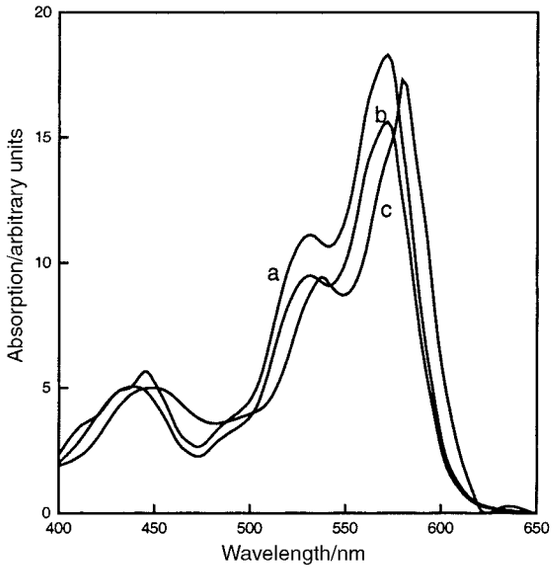

Fig. 5 Absorption spectra of T-PTCA7(a); T-PTCA4(b); T-PTCA6(c) in acetone (10^{-5} M).

identical, and this is due to their very similar structures. The expected broadening of their absorption bands compared to T-PTCA4, which could be measured by the half-height width of the longest absorption band,[4b] was not displayed. As seen in Fig. 5, the shapes of the absorption spectra of the T-PTCA series are very similar to each other. They all have high molar extinction coefficiency. The extension of the π-system in the bay region induces a dramatic bathochromic shift compared with RPTCA and PPDCA, non-substituted perylenes in the bay region. In comparison with T-PTCA5 and T-PTCA6, the maximum absorption wavelengths of compounds T-PTCA2, T-PTCA4, T-PTCA7 and T-PTCA8 are similar, a little shorter than the former. This indicated that the linking of two π-systems through a single bond did not result in much alteration of the UV/Vis spectra. Only an appreciable overlap of the chromophore induced strong absorption at longer wavelengths.[17]

The absorption spectral data for the T-PTCA series in different solvents are shown in Table 2. The maximum absorption wavelengths were longer in chloroform than in acetone for all the perylene derivatives. This showed that the less polar solvents are beneficial for the bathochromic shifts for the perylenes, *i.e.* they produce a larger bathochromic shift.

The shapes of the absorption spectra of compound T-PTCA4 and T-PTCA5 in solution and on solid film are very similar. However, the spectra of T-PTCA2, T-PTCA7, T-PTCA8 and T-PTCA6 on solid film show only an unstructured broad band. It is of interest that the differences of the maximum absorption wavelength of T-PTCA4, T-PTCA2 and T-PTCA5 between solution and solid film are small, yet remarkably bathochromic shifts occur for compounds T-PTCA7, T-PTCA8 and T-PTCA6 in acetone and on solid film: 60, 50 and 40 nm, respectively. This phenomenon could not be explained only by the π interaction or intermolecular overlap in the solids. Compared with T-PTCA4 and T-PTCA2, the T-PTCA7, T-PTCA8 have bulky groups at the nitrogen atoms, which could lower the intermolecular interaction.[9b] Since–COOH or –OH groups are present in compounds T-PTCA7, T-PTCA8 and T-PTCA6, we believe that, at least in part, changes in the structures and maximum

Table 2 The solvent effect on the absorption spectra of compounds synthesized

Dyes	T-PTCA4	T-PTCA2	T-PTCA7	T-PTCA8	T-PTCA5	T-PTCA6
$CHCl_3$	578.6	583.4	586.2	585.6	590.2	595.0
Acetone	569.8	565.2	569.8	568.6	575.0	579.6

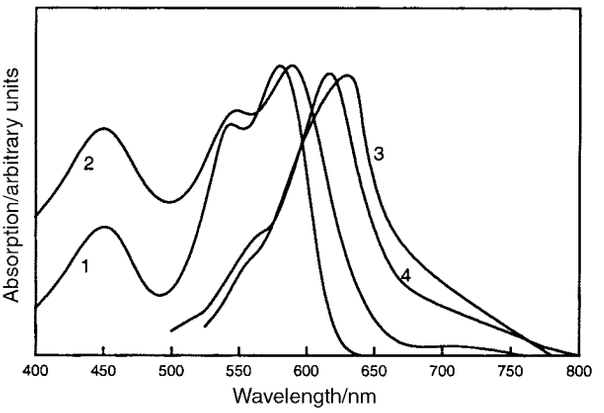

Fig. 6 Absorption spectra of T-PTCA4(1); T-PTCA5(2); T-PTCA7(3); T-PTCA6(4) on solid film.

Table 3 Fluorescence data for the compounds in solution (10^{-5} M)

Compound (Solvent)	λ_{ex}/nm	λ_{em}/nm	Relative intensity
T-PTCA4 ($CHCl_3$)	578.6	613.1	51.71
T-PTCA2 ($CHCl_3$)	583.4	613.4	40.83
T-PTCA7 (acetone)	569.8	603.4	52.17
T-PTCA8 (acetone)	568.6	601.4	57.80
T-PTCA5 (acetone)	575.6	607.4	0.211
T-PTCA6 (acetone)	579.6	613.9	0.152

absorption of the absorption spectra indicate greater hydrogen bonding than explained by the small influence of intermolecular π-conjugation. Because the low concentrations of the solution and polar solvents both do not favor hydrogen bond formation,[5b,5c] no excimers or oligmers were observed in the UV-Vis absorption. However, the intermolecular interaction between –OH and –H is very strong for compounds T-PTCA7, T-PTCA8 and T-PTCA6 on solid film, so large bathochromic shifts occurred (Fig. 6).

Except for T-PTCA5 and T-PTCA6, the other T-PTCAs are highly fluorescent, and high fluorescence quantum yields are obtained for the T-PTCA series. The results of fluorescence spectra of the T-PTCA series (Table 3) exhibit the typical mirror symmetry between absorption and emission bands. This indicates that little structural rearrangement occurs between the ground and the excited state of the compound. The characteristic Q bands of perylene, *i.e.* they show a singlet at around 600 and 610 nm together with a shoulder at around 659 and 660 nm in the Q band region (500–800 nm), were observed from their emission spectra. For compounds T-PTCA5 and T-PTCA6, their absorption in the visible region was strong, but the fluorescence emission was very weak, as seen in Table 3 and Fig. 7.

Photosensitization on SnO_2 nanoporous film

The absorption spectra of sensitized and unsensitized SnO_2 electrodes were determined (shown in Fig. 8). The spectra show that the unsensitized electrode (bare SnO_2 film) exhibits the fundamental absorption at 306 nm (band gap energy, 3.8 eV[4]) in the ultraviolet region. However, the multi-chromophoric dye sensitized electrode has a strong absorption in the UV and visible region. It indicates that the OXZ-PER dye has been adsorbed onto the nanoporous ITO/SnO_2 electrode. The nature of the interaction leading to adsorption of the dye on the surface may be the interaction between the carbonyl group and SnO_2 resulting from either bonding electrostatically or forming an ester linkage by a hydrolysis reaction with a Sn–OH.[4] This is similar with that between a carboxy group and TiO_2. The absorption peaks at 340, 439 and 529 nm indicate that there is little or no interaction between the oxadiazole and

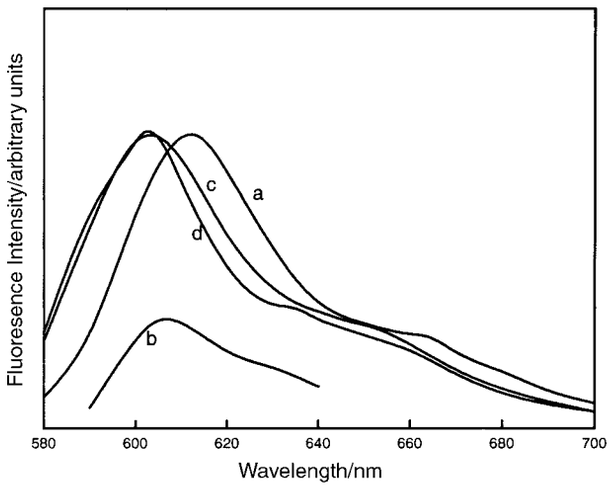

Fig. 7 Fluorescence emission spectra of compounds T-PTCA4 in $CHCl_3$(a); T-PTCA5 in acetone(b); T-PTCA7 in acetone(c); T-PTCA8 in acetone(d).

perylene chromophores even in the adsorbed state. Thus the responding photocurrent of the nanocrystalline SnO_2 sensitization by the novel multi-chromophoric OXZ-PER dye could cover a wide range of absorption.

Photocurrent–voltage characteristics under white light irradiation and action spectra of the photocurrent were measured with the two-electrode system shown in Fig. 9 to characterize the photoenergy conversion efficiency. Fig. 9 shows the photocurrent action spectra of the sensitized and unsensitized SnO_2 electrode. As shown in Fig. 9, the open circuit voltage (V_{oc}) and short-circuit photocurrent (J_{sc}) of the sensitized electrode by OXZ-PER dye were 0.17 V and 180 mA (*i.e.* 900 mA cm^{-2}), respectively. The fill factor (FF) was 0.34.[21] The dye sensitized nano-SnO_2 electrode showed relatively large J_{sc} although V_{oc} was relatively small. The photoresponse was drastically broadened to the visible light region, covering a wide range of spectrum (310 to 700 nm). The photocurrent of the unsensitized electrode (ITO/SnO_2) was very low around the 400 nm region and decreased to almost zero at 500 nm. A little photocurrent generated by the light with wavelength over 400 nm may be related to the surface states or inner localized states of bare SnO_2 nanostructured film. These surface states or inner localized states may absorb a photon of energy smaller than its energy gap and make a contribution to produce very small photocurrent in this wavelength region. When sensitized by OXZ-PER, the maximum IPCE of the cell in the UV region reached 12% (at 370 nm). In the visible region the maximum IPCE at 540 nm reached 10.5%. The photocurrent was drastically broadened to a wide visible light region covering 400 to 650 nm. Since IPCE values are not corrected for the loss owing to incident light scattering by the glass support, the energy conversion at the maximum IPCE for the dyed nano-SnO_2 should in fact be higher. After one month storage in dark, the cell sensitized by OXZ-PER still shows short-circuit photocurrent of 500 mA cm^{-2}.

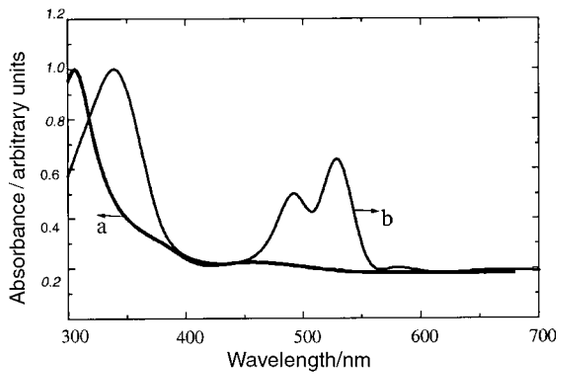

Fig. 8 Absorption spectra of SnO_2 nanostructured porous film deposited on conducting glass unsensitized (curve a) and dye-sensitized by OXZ-PER (curve b).

The above special sensitization effect of photoelectrical performance of the cell can be explained in terms of the band models shown in Fig. 2. The band bending resulting from the organic–inorganic p–n heterojunction, facilitates electron injection from the excited state of OXZ-PER into the conduction band of the SnO_2 semiconductor. The band energies of SnO_2,[4] oxadiazole unit[14,19] and perylene unit[5,15] can be taken from the appropriate references. The LUMO level of the oxadiazole unit and perylene unit in OXZ-PER dye is higher than the conduction band of SnO_2. This means that the excited level (LUMO) of the oxadiazole unit and perylene unit matches the conduction band position of nanocrystalline SnO_2. When irradiating under white light, the electrons were excited from the HOMO orbital (−5.9 eV) to the LUMO orbital (−3.9 eV) of the perylene unit and then injected from the LUMO orbital of the perylene unit into the conduction band of SnO_2 (−4.73 eV). For the oxadiazole unit, a similar electron transfer exists. However, the electrons of the LUMO orbital of oxadiazole unit have two possible approaches to inject into the conduction band of SnO_2. One is direct electron injection from the LUMO orbital of the oxadiazole unit (−2.5 eV) into the conduction band of SnO_2. Another is indirect electron injection from the LUMO orbital of the oxadiazole unit *via* the LUMO orbital (−3.9 eV) of the perylene unit into the conduction band of SnO_2. That is, there exist the energy transfer and/or electron transfer from the oxadiazole unit to the perylene unit at first. Then, the electrons inject from the LUMO orbital of the perylene unit into the conduction band of SnO_2. In addition, a redox electrolyte (I_3^-/I^-) is used to mediate charge transfer between the electrons and to regenerate the sensitizer. As a consequence, a drastic photoresponse with wide spectral sensitization (from 310 to 700 nm) is achieved. In fact, the role of SnO_2 in the liquid junction cell based on the OXZ-PER is merely to conduct the injected electrons.

Because of the improved solubility of the T-PTCA series in common organic solvents, the adsorption of dyes onto the SnO_2 film should be improved. The absorption spectra of the T-PTCA7 dye sensitized SnO_2 electrode were very similar to that of dye film. This means that there is little or no interaction between chromophores connected with saturated covalent bonds in their ground state even in the adsorbed state, so that their individual absorption characteristics should be maintained for T-PTCA7. On the other hand, because of steric constraints, the carboxylic acid groups on the phenyl ring are oriented perpendicular to the perylene ring system. The poor photosensitization (a relative small photocurrent density of

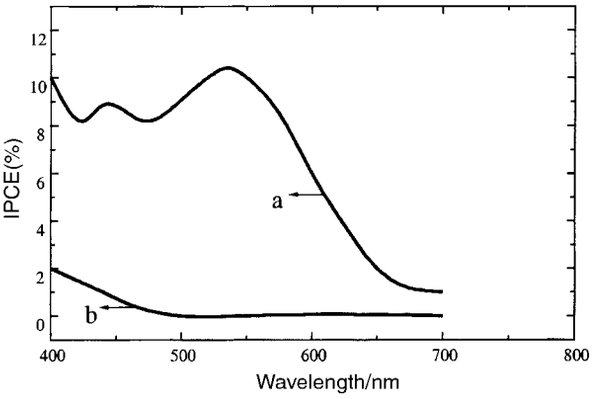

Fig. 9 Photocurrent action spectra of OXZ-PER dye-sensitized (curve a) and unsensitized SnO_2 porous films (curve b). Insert figure: photovoltage–current characteristics of the cell based on dye-sensitized SnO_2 nanostructured electrode.

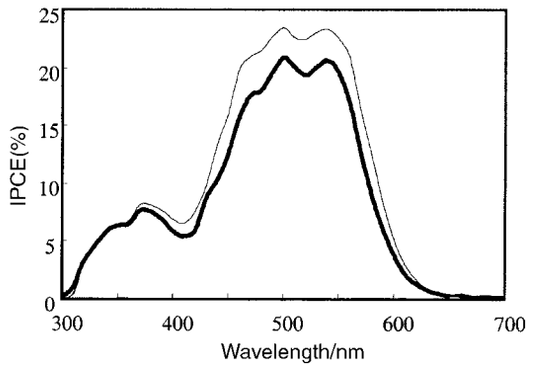

Fig. 10 Perylene T-PCTA7 adsorbed on nanoporous SnO_2 electrode.

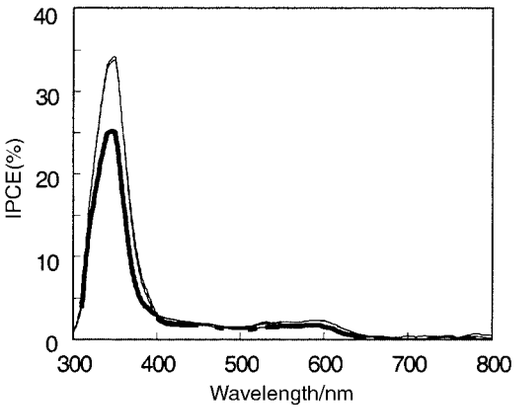

Fig. 11 IPCE spectra of perylene T-PCTA8 adsorbed on nanoporous TiO_2 electrode.

~ 100 mA cm^{-2}) obtained for this kind of dye (T-PTCA series) may be related to its orientation on the surface of the SnO_2 particles. When sensitized by T-PTCA7, the maximum IPCE of the cell in the visible region reached 24% (at 500 nm). The photocurrent was drastically broadened to a wide visible light region covering 400 to 600 nm, as shown in Fig. 10. As the comparison system, the photocurrent response of the T-PTCA8 dye sensitized nano-structured TiO_2 electrode was determined, which were shown in Fig. 11. As seen in Fig. 11, the photon-to-current quantum yields in the visible region for T-PTCA8 sensitized TiO_2 film were very small. This may result from the poor adsorption of the dye on the surface of the TiO_2. The results indicated that only the carboxylic acid group is effective for the adsorption onto the surface of SnO_2 and TiO_2 nanoparticles. The other groups such as hydroxy would influence the adsorption, so consequently result in a poor photosensitization. In Fig. 10 and 11, the photoresponses of the cells shown by the thick lines were obtained after two hours exposure to white light (200 W Hg lamp). The results show relative better photostability of the perylenes synthesized in the study.

In addition, due to the good solubility of the T-PTCA series compounds in organic solvents, the oxidation potential of these compounds can be obtained by the measurements of solution electrochemistry. The oxidation potential of a commercially available *N*,*N*′-bis(2,5-di-*tert*-butylphenyl)perylene-3,4:9,10-tetracarboxydiimide is +1.66 V *vs.* SCE in CH_2Cl_2. The very positive oxidation potential is thermodynamically capable of driving the water oxidation reaction at appropriate pH. The oxidation potential of T-PTCA series synthesized in this study were between +1.00 and +1.60 V (SCE), which should be a substantial over-potential for water oxidation (+0.63 V *vs.* SCE at pH 7).[4] The perylene dyes presented here may be useful in water-splitting dye-sensitized solar cells.

In summary, we have found a novel route to design highly efficient sensitizers for Grätzel-type solar cells, which can avoid the complication of doping. Two series of new multi-chromophoric perylene-3,4:9,10-tetracarboxylic dianhydride dyes for solar cell sensitizer have been synthesized. One series consists of oxadiazole or naphthaldicarboximides linked by perylene units as *N*,*N*′-substituted chromophores. The other series has four substituents in the bay-region of the perylene core besides *N*,*N*′-substituents. The latter series of T-PTCA compounds have surprisingly good solubility in common organic solvents, in addition to good photo- and thermal-stability. In the dye sensitized SnO_2 system, a wide spectral photoresponse (from 310 to 700 nm) was observed for these novel multi-chromophoric dyes. In addition, the sensitization is dependent on the energy match of the energy bands of the semiconductor and the redox potentials of the segments in such assembled dyes.

Acknowledgements

This project was supported by NSFC/China and partially sponsored by the Shanghai Scientific Committee. Authors are indebted to Professor Dr K. Müllen (MPI for Polymer Research, Mainz/ Germany) and Professor K. C. Chen (ECUST, Shanghai/ China) in the synthesis of the compounds.

References

1 B. O'Regan and M. Grätzel, *Nature (London)*, 1991, **353**, 737.
2 M. K. Nazeeruddin, A. Kay, I. Rodicio, R. Humphry-Baker, E. Müller, N. Vlachopoulos and M. Grätzel, *J. Am. Chem. Soc.*, 1993, **115**, 6382.
3 O. Kohle, M. Grätzel, A. F. Meyer and T. B. Meyer, *Adv. Mater.*, 1997, **9**, 904.
4 (*a*) D. Schlettwein, D. Wōhrle, E. Karmann and U. Melville, *Chem. Mater.*, 1994, **6**, 3; (*b*) S. Ferrere, A. Zaban and B. A. Gregg, *J. Phys. Chem. B*, 1997, **101**, 4490.
5 (*a*) D. Dotcheva, M. Klapper and K. Müllen, *Macromol. Chem. Phys.*, 1994, **195**, 1905; (*b*) H. Quante, Y. Geerts and K. Müllen, *Chem. Mater.*, 1997, **9**, 495; (*c*) H. Icil, S. Icli and C. Sayil, *Spectrosc. Lett.*, 1998, **31**(8), 1643; (*d*) F. Würthner, C. Thalacker and A. Sautter, *Adv. Mater.*, 1999, **11**, 754.
6 M. P. O'Neil, M. P. Niemczyk, W. A. Sves, D. Gosztola, G. L. Gaines and M. R. Wasielewski, *Science*, 1992, **257**, 63.
7 R. Gvishi, R. Reisfeld and Z. Burshtein, *Chem. Phys. Lett.*, 1993, **213**, 338.
8 R. L. Rill and Z. R. Liu, Florida State University, USA, WO 97 25,314, 1997.
9 (*a*) H. Langhals, S. Sprenger and M.-T. Brandherm, *Liebigs Ann. Chem.*, 1995, 481; (*b*) Y. Nagao, T. Naito, Y. Abe and T. Misono, *Dyes Pigm.*, 1996, **32**, 71.
10 M. Hiramoto, Y. Kishigrami and M. Yokoyama, *Chem. Lett.*, 1990, 119.
11 C. W. Tang, *Appl. Phys. Lett.*, 1986, **48**, 183.
12 H. H. Deng, Z. H. Lu, Y. C. Shen and H. J. Xu, *Chem. Phys.*, 1998, **231**, 95.
13 R. Amadelli, R. Argazzi, C. A. Bignozzi and F. Scandola, *J. Am. Chem. Soc.*, 1990, **112**, 7099.
14 R. Memming, *Electrochim. Acta*, 1980, **25**, 77.
15 H. Quante, P. Schlichting, U. Rohr, Y. Geerts and K. Müllen, *Macromol. Chem. Phys.*, 1996, **197**, 4029.
16 K. D. Shimizu, T. M. Dewey and J. Rebek. Jr., *J. Am. Chem. Soc.*, 1994, **116**, 5145.
17 H. Langhals and W. Jona, *Angew. Chem., Int. Ed.*, 1998, **37**, 952.
18 L. Zhang, E. Gao, M. Yang, X. Qiao, Y Hao, S. Cai, F. Meng and H. Tian, *Wuli Huaxue Xuebao*, 1999, **15**, 293.
19 F. Cacialli, X. C. Li, R. H. Friend, S. C. Moratti and A. B. Holmes, *Synth. Met.*, 1995, **75**, 161.
20 H. Tian, T. Xu, Y. Zhao and K. Chen, *J. Chem. Soc., Perkin Trans. 2*, 1999, 545.
21 The fill factor FF = E_{max}/ (J_{sc}· V_{oc}), where E_{max} is the maximum output power of the cell, J_{sc} is the short circuit current, V_{oc} is the open-circuit voltage.